Zero-field optical detection of magnetic resonance on a metastable sulfur-pair-related defect in silicon: Evidence for a Cu constituent

A. M. Frens, M. T. Bennebroek, and J. Schmidt
Centre for the Study of Excited States of Molecules, Huygens Laboratory, University of Leiden, P.O. Box 9504, NL-2300 RA Leiden, The Netherlands

W. M. Chen and B. Monemar
Department of Physics and Measurement Technology, Material Science Division, Linköping University, S-581 83 Linköping, Sweden

(Received 7 February 1992; revised manuscript received 27 July 1992)

A metastable complex defect in S-doped silicon has been studied with zero-field optically-detected magnetic-resonance (ODMR) spectroscopy. The defect shows two characteristic photoluminescence (PL) spectra S_A and S_B, corresponding to two different geometric configurations 1 and 2. The PL spectra in both cases originate from excited-state triplet bound excitons in the neutral charge state of the defect. Previous X-band ODMR studies for S_A and S_B show broad spectra with unresolved hyperfine interaction. In zero-field ODMR the linewidth is reduced to about 50 MHz for S_A (100 MHz for S_B), and the second-order hyperfine structure of an $I=\frac{3}{2}$ nucleus is resolved, partly with the help of a double-resonance technique. The zero-field splitting parameters of the triplet states (i.e., the principal D-tensor components) are determined as $D_{xx}=-2905$, $D_{yy}=-705$, and $D_{zz}=3610$ MHz for S_A, and $D_{xx}=-1295$, $D_{yy}=-180$, and $D_{zz}=1475$ MHz for S_B. The hyperfine splitting is determined as $A=175$ MHz for both S_A and S_B, whereas the quadrupole constant $P_{z'z'}$ has a value 10–20 MHz for S_A and a substantially larger value, 30–40 MHz for S_B. The $I=\frac{3}{2}$ nucleus at the core of the defect is tentatively identified as Cu. The conclusion about the different quadrupole interaction for S_A and S_B from these data agrees with previous ODMR X-band data in a magnetic field, which also show a different configuration (of the Cu atom) in the excited triplet states of S_A and S_B. It is tentatively concluded from these data that the metastability of this defect is connected to a change of the site of the Cu atom with respect to its surroundings in the silicon lattice.

I. INTRODUCTION

Recently a sulfur-related complex defect in silicon has attracted much attention due to its interesting configurational metastability.[1–4] Two photoluminescence spectra S_A and S_B, characteristic for configurations 1 and 2, respectively, with zero-phonon lines at 0.968 eV (S_A^0) and at 0.812 eV (S_B^0) at low temperature, were shown to originate from photoexcited triplet states.[2] These spectra have been identified with the recombination of an exciton bound to this defect in its neutral charge state. Conversion between the two configurations, identified by S_A and S_B, takes place either by light ($S_A \rightarrow S_B, T<40$ K) or by thermal annealing ($S_B \rightarrow S_A, T>40$ K).[3] Recently it has been suggested that the sulfur pair is involved in the defect since the energy splitting between S_A^0 and S_B^0 is the same as between the $1s(A_1^+)$ ground and the $1s(E^-)$ excited states of the neutral sulfur pair.[4,5] It is assumed that in addition to the two sulfur atoms, which occupy nearest-neighbor substitutional sites, another impurity or an intrinsic defect is present in the complex.

A study of the two triplet states with optically-detected magnetic resonance (ODMR) at X-band (9.23-GHz) frequencies showed unusual broad and structureless lines with a width of approximately 25 mT. From these experiments the symmetry for configuration 2 was found to be monoclinic I but, owing to the broad ODMR lines, it was not possible to determine the exact zero-field parameters and the symmetry of configuration 2. Implantation with the ^{33}S ($I=\frac{3}{2}$) isotope showed that the large linewidth is not due to hyperfine interaction with a sulfur nucleus.[6,7]

In this work we report the results of ODMR experiments on both the S_A^0 and S_B^0 excited triplet states in zero-magnetic field, from which we conclude that a Cu atom is involved in this S-related defect. This conclusion is based on an analysis of the line shape of the zero-field transitions in terms of second-order hyperfine interaction with a nuclear spin $\frac{3}{2}$. The result illustrates some attractive features of zero-field ODMR spectroscopy for the study of defects in semiconductors. First the technique of double-resonance spectroscopy is found very useful in observing transitions between levels having either equal populations or radiative decay rates. Second hyperfine interactions, that are not resolved in the presence of a magnetic field, reveal themselves in the zero-field spectra and allow us to identify an impurity atom in a complex defect without the need to resort to isotope enriched material or to electron-nuclear double-resonance (ENDOR) techniques.

II. EXPERIMENT

The samples used in this work were cut from single crystalline float-zone p-type ingot material (6000 Ωcm). The sulfur doping was done by high-temperature diffusion. The silicon crystal together with 1 mg (99.999% purity) S and 5 mg Si powder were put in a quartz ampoule which was evacuated. In this ampoule there was no direct contact between the crystal and the powders. After 40 h of diffusion at 1200 °C the ampoule was dropped quickly in water. A second step was to anneal the sample in a flame (natural gas and air) for a few seconds followed by a rapid quench in a mixture of ethylene glycol and water (50/50).

For the conventional (single-resonance) ODMR experiments the sample was placed in a tunable reentrant cavity.[8,9] In the double-resonance experiments a shorted coaxial line was used to apply microwaves at two different frequencies to the sample. The microwaves were generated by sweep generators (Hewlett Packett 8690B) and amplified by Traveling Wave Tube amplifiers (Varian VA 1350G). The resonators containing the sample were immersed in liquid helium pumped down to a pressure corresponding to 1.2 K. Some of the experiments were carried out at 4.2 K. The excitation light was provided by a Nd:YLF (yttrium-landhanum-fluoride) laser operating at 1047 nm (CVI Yag max). This excitation wavelength turns out to be very advantageous for ODMR experiments in silicon, since no free carriers are created, which would give rise to large cyclotron resonance background signals.[10] In the case of the S_B transitions the luminescence was detected through a 1500-nm long-wave-pass (LWP) optical filter whereas a 1200-nm LWP and a 1500-nm short-wave-pass filter were used in the case of the S_A emission. The luminescence was detected with a liquid-nitrogen-cooled germanium detector (North Coast EO 817S).

III. RESULTS

The principles of zero-field ODMR are the following. Optical pumping with the 1047-nm output of the Nd:YLF laser is required to populate the excited triplet state of the sulfur-related defect. The microwave power is applied to produce changes in the populations of the different, nondegenerate, spin levels. The optical detection is based on changes in the PL intensity because of the different radiative decay rates for the different spin states. In practice the zero-field spectra are recorded by slowly scanning the microwave frequency with amplitude modulation of the microwave power and synchronous detection of the PL intensity. In curves (a) and (b) of Fig. 1 we show the ODMR signals so obtained for the transitions T_y-T_z (4.3 GHz) and T_x-T_z (6.5 GHz) of the S_A triplet state for high- and low-microwave power, respectively. In curves (a) and (b) of Fig. 2 we present the signals of the transitions T_x-T_y (1.2 GHz) and T_y-T_z (1.7 GHz) for S_B. In contrast to S_A the line shapes of S_B do not change with microwave power.

The ODMR detection technique just described failed for observing the T_x-T_y (2.2-GHz) transition in S_A and the T_x-T_z (2.85-GHz) transition in S_B because the two

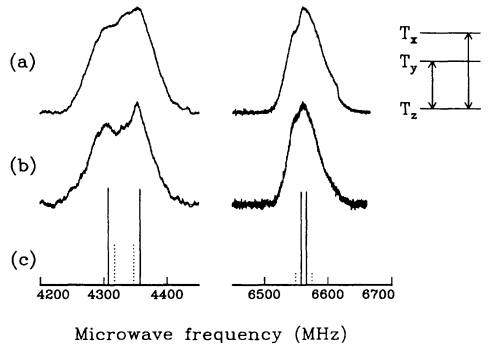

FIG. 1. (a) and (b) The T_x-T_z and T_y-T_z ODMR transitions for the S_A triplet state at high (±200 mW) and low (±10 mW) microwave power. (c) The calculated positions for the forbidden (dashed lines) and allowed (solid lines) transitions as obtained from the fitting procedure with the aid of the spin Hamiltonian [Eq. (1)]. The length of the sticks indicates the relative values of the transition probabilities.

sublevels involved have the same radiative decay rate, as we will prove in a forthcoming paper.[11] For the detection of these transitions we had to resort to a double-resonance experiment. To illustrate this technique we shall discuss the case of the S_A triplet. Here we first pump the T_y-T_z transition with cw microwaves at a fixed frequency. When using a saturating microwave power the populations of the two levels are equalized and become $(N_y+N_z)/2$. To make the T_x-T_y transition visible we subsequently scan a saturating amplitude modulated microwave field through the T_x-T_y resonance region and detect again synchronously in the photoluminescence intensity. This second microwave field will change the population of T_x, T_y, and T_z to $(N_x+N_y+N_z)/3$ and since the radiative decay rate of T_z is different from T_x and T_y this will lead to a change in photoluminescence intensity. In Fig. 3(a) we present the result of such an experiment on the T_x-T_y transition for the S_A triplet, where the cw microwave field is fixed at 4300 MHz (β) and at 4350 MHz (α), respectively, while the amplitude modulated microwaves are scanned through the 2.2-GHz region. In Fig. 2(c) the result of a similar experiment on the T_x-T_z transition for the S_B triplet is presented.

The double-resonance experiment allowed us to prove that the T_x-T_y and the T_y-T_z transitions of the S_A triplet consists of two components as shown in Fig. 3. Here we see that when using a cw microwave field at 4350 MHz we find a transition at 2200 MHz (α) whereas a transition at 2260 MHz (β) shows up when applying microwaves at 4300 MHz [Fig. 3(a)]. Alternatively when utilizing amplitude modulated microwaves fixed at 2200 or 2260 MHz we find two transitions at 4350 MHz (δ) and 4300 MHz (γ), respectively [Fig. 3(b)]. The double-resonance experiments also allowed us to determine the linewidth of the transitions to be about 50 MHz. This value is considerably smaller than the linewidth of 700 MHz (25 mT) observed in the X-band ODMR experiments. This reduction of the linewidth is caused by the quenching of the hyperfine interaction in first order in zero-magnetic field.

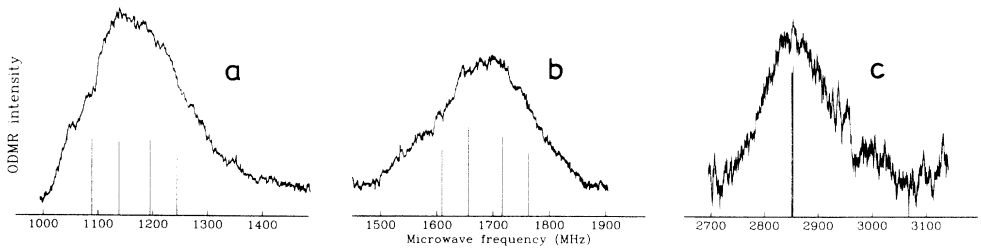

FIG. 2. The ODMR transitions for the S_B triplet state together with the calculated line positions. (a) and (b) The conventional transitions. (c) The double-resonance transition.

For the S_B triplet similar experiments were performed but here no splitting but only broad (200-MHz) structureless lines, could be observed. The origin of this difference will be explained in Sec. IV.

IV. DISCUSSION

In this section we shall first concentrate on the S_A triplet state where we have found that two of the three zero-field ODMR transitions exhibit a remarkable doublet structure. For instance, for the T_y-T_z transition this splitting amounts to 50 MHz and is directly observable. For the T_x-T_y transition the splitting is larger (60 MHz) but it only can be made visible via a double-resonance experiment. We shall argue that this structure can be understood in terms of second-order hyperfine interaction with an $I=\frac{3}{2}$ nuclear spin, in all probability from a copper atom involved in the S-related complex. In the second part we turn to the case of S_B and we will demonstrate that the line shapes observed here can be understood by a similar model.

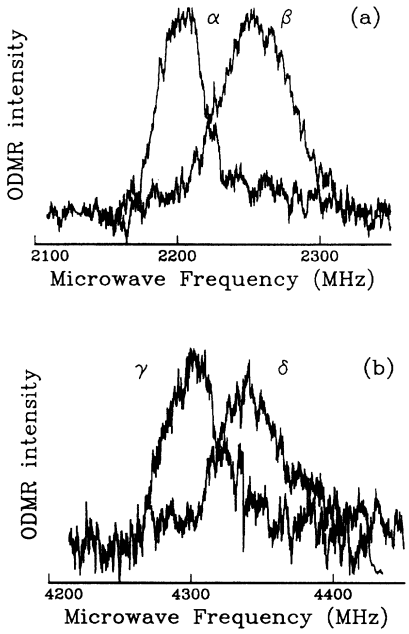

FIG. 3. The double-resonance ODMR transitions for the S_A triplet state. (a) Transitions α and β are obtained by application of 4350- and 4300-MHz cw microwaves, respectively, while scanning amplitude modulated microwaves in the 2.2-GHz region. (b) Transitions γ and δ are found by fixing the amplitude modulated microwaves at 2260 and 2200 MHz, respectively, while scanning the cw microwaves in the 4.3-GHz region.

The assumption that second-order hyperfine interaction is responsible for the line shape of the zero-field transitions of the S_A triplet is based on the fact that the hyperfine interaction changes from a first-order to a second-order effect when going to zero-magnetic field and on the observation that the linewidth is strongly reduced when turning off the magnetic field.[12] When thinking about the nuclear species that could be responsible for the observed doublet structure we can first of all exclude the possibility that it arises from a nuclear spin $I \geq \frac{5}{2}$ because this would lead to a splitting into three or more components of the ODMR lines. The ^{29}Si nuclei ($I=\frac{1}{2}$) cannot cause a splitting of the triplet sublevels (Kramer's theorem) but merely a shift of their energy. However the ratio of the natural abundances of ^{29}Si (4.7%) and ^{28}Si (95.3%) is not at all compatible with the 1:1 intensity ratio of the two components in the doublet structure. The possibility that a nuclear spin $I=1$ is involved can also be discarded because atoms like ^{14}N, ^{6}Li, and ^{2}D are improbable impurities. Further it has been demonstrated that $S(^{33}\text{S}, I=\frac{3}{2}$ abundance 0.76%) is not responsible because in samples implanted with ^{33}S no effect was observed in the ODMR linewidth. This leaves the nuclear spin $I=\frac{3}{2}$ with Cu (^{63}Cu, $I=\frac{3}{2}$; $g_n=1.484$; $Q=-0.356\times10^{-45}$ C cm^2, abundance 69.1% and ^{65}Cu $I=\frac{3}{2}$; $g_n=1.588$; $Q=-0.312\times10^{-45}$ C cm^2, abundance 30.9%) as the most probable candidate. It is known that Cu is a rapid diffuser in silicon[13] and is present in materials subject to the quenching procedure used for our samples.

In our treatment we neglect the difference in the nuclear g values and quadrupole moments of the two copper isotopes and we use a Hamiltonian for describing the interaction between the electron spin system and a single nuclear spin $I=\frac{3}{2}$ of the following form:

$$H=H_{ss}+H_Q+H_{\text{HF}}=\mathbf{S}\cdot\vec{D}\cdot\mathbf{S}+\mathbf{I}\cdot\vec{P}\cdot\mathbf{I}+\mathbf{S}\cdot\vec{A}\cdot\mathbf{I}\ . \quad (1)$$

Here the first term describes the zero-field splitting of the electron spins induced by the spin-orbit interaction and spin-spin interactions. In its principal axis system, denoted by x,y,z, H_{ss} can be written:

$$H_{ss}=D_{zz}S_z^2+D_{yy}S_y^2+D_{xx}S_x^2\ . \quad (2)$$

H_{ss} is diagonal on the basis of the triplet functions T_z, T_y, and T_x. These functions are linear combinations of the eigenfunctions of the S_z operator:

$$T_x=\frac{1}{\sqrt{2}}(|+1\rangle-|-1\rangle)\,,$$
$$T_y=\frac{i}{\sqrt{2}}(|+1\rangle+|-1\rangle)\,, \tag{3}$$
$$T_z=|0\rangle\,.$$

The functions have the property

$$S_xT_y=-S_yT_x=iT_z\,,$$
$$S_uT_u=0,\quad u=x,y,z\,. \tag{4}$$

The result is that matrix elements of the type $\langle T_u|H_{\rm HF}|T_u\rangle=0$ and the hyperfine interaction reduces to a second-order effect.

The second term H_Q of (1) represents the quadrupole splitting of the spin states of the $I=\frac{3}{2}$ nucleus. Its principal axis system x',y',z' is determined by the electric-field gradient at the nucleus and H_Q can be written as

$$H_Q=P_{z'z'}I_{z'}^2+P_{y'y'}I_{y'}^2+P_{x'x'}I_{x'}^2$$
$$=\tfrac{1}{2}P_{z'z'}[3I_{z'}^2-I(I+1)+\eta(I_{x'}^2-I_{y'}^2)] \tag{5}$$

with

$$\eta=\frac{P_{x'x'}-P_{y'y'}}{P_{z'z'}}\quad(0<\eta<1)\,.$$

In the second form of H_Q the parameter η is a measure for the deviation from axial symmetry of the electric-field gradient at the position of the nucleus. If $\eta=0$, H_Q is diagonalized by the nuclear spin functions $m_I=\pm\frac{3}{2}$ and $m_I=\pm\frac{1}{2}$.

For the present purpose we would need the eigenenergies and the directions of the principal axes of H_Q. These quantities are not known. For simplicity we shall take x',y', and z' to coincide with the principal axis system of the zero-field tensor, but the choice whether z' is parallel to x,y, or z is free. This problem will be discussed in the analysis of the spectra (vide infra). Further we estimate the quadrupole splitting of the Cu nuclear spin to be in the order of 0–30 MHz.[14]

The last term $H_{\rm HF}$ describes the hyperfine interaction between the electron spin and the nuclear spin systems. A rough estimate of $A=200$ MHz for the hyperfine interaction can be obtained from the X-band ODMR experiments of Chen *et al.*[6,7] Since no indication was found of an anisotropy of A we assume that $H_{\rm HF}$ can be written as

$$H_{\rm HF}=A(S_xI_x+S_yI_y+S_zI_z)\,. \tag{6}$$

The spin functions which diagonalize $H_{ss}+H_Q$ for $\eta=0$ are $|T_u;m_I\rangle(u=x,y,z;m_I=\pm1/2,\pm3/2)$. Hence if the term $H_{\rm HF}$ were absent each of the three electron

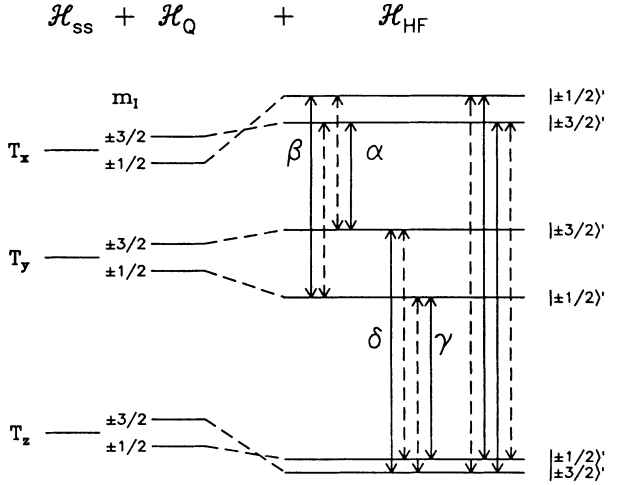

FIG. 4. The calculated positions of the triplet sublevels with the quadrupole z' axis along the x axis of the D tensor for S_A. The labels $|\pm m_I\rangle'$ refer to the $|T_u;m_I\rangle'$ eigenfunctions in Tables III and IV. The labels α,β,γ, and δ correspond to the observed transitions in Fig. 3. Schematically the same figure applies for S_B.

levels would consist of two components with energies

$$U\pm3\frac{P_{z'z'}}{2}\left[1+\frac{\eta^2}{3}\right]^{1/2}\,,$$

with (7)

$$\eta=\frac{P_{y'y'}-P_{x'x'}}{P_{z'z'}}\ \text{and}\ U=-D_{xx},-D_{yy},-D_{zz}\,,$$

as indicated in Fig. 4. The zero-field signals would then correspond to transitions of the type $|T_z;\pm\frac{1}{2}\rangle\leftrightarrow|T_y;\pm\frac{1}{2}\rangle$ and $|T_z;\pm\frac{3}{2}\rangle\leftrightarrow|T_y;\pm\frac{3}{2}\rangle$ where the nuclear spin state is conserved. In this situation the nuclear components of each electron transition would coalesce since the nuclear spins do not "feel" the electron spins. The presence of the hyperfine term causes an admixture of states of the different T_u manifolds. This will lead to a second-order shift of the energies and the possibility of "forbidden" transitions, i.e., to a relaxation of the $\Delta m_I=0$ selection rule of the zero-field transitions, as can be seen from Table I where we present the Hamiltonian matrix of Eq. (1).

Diagonalization of the Hamiltonian matrix of Table I and comparison of the resulting transition frequencies with the observed line shapes reveal the values for D_{ii}, $P_{z'z'}$, η, and A. The best fit to the spectra was obtained by the set of parameters given in Table II. In Table III we give the eigenenergies and eigenfunctions of the levels for S_A. It is seen that for the T_x and T_z manifolds typically 20% of $m_I=\pm\frac{1}{2}$ character is mixed into the $m_I=\pm\frac{3}{2}$ levels and vice versa, whereas for the T_y doublet this is in the order of 5%. The position of the sublevels and the possible allowed ($\Delta m_I=0$) and forbidden ($\Delta m_I=\pm1$) transitions are indicated in Fig. 4 by solid and broken lines, respectively.

In Fig. 1(c) we show in a stick diagram the calculated

TABLE I. The Hamiltonian matrix of Eq. (1) where we have used the abbreviations: $\alpha=\frac{1}{2}\sqrt{3}, H=\eta P_{z'z'}\sqrt{\frac{3}{2}}$, and $Q=\frac{3}{2}P_{z'z'}$.

	T_x				T_y				T_z			
H	$+\frac{3}{2}$	$-\frac{3}{2}$	$+\frac{1}{2}$	$-\frac{1}{2}$	$+\frac{3}{2}$	$-\frac{3}{2}$	$+\frac{1}{2}$	$-\frac{1}{2}$	$+\frac{3}{2}$	$-\frac{3}{2}$	$+\frac{1}{2}$	$-\frac{1}{2}$
$\lvert T_x;+\frac{3}{2}\rangle$	$-D_{xx}+Q$			H	$-3/2iA_{zz}$						αA_{yy}	
$\lvert T_x;-\frac{3}{2}\rangle$		$-D_{xx}+Q$	H			$3/2iA_{zz}$						$-\alpha A_{yy}$
$\lvert T_x;+\frac{1}{2}\rangle$		H	$-D_{xx}-Q$				$-1/2iA_{zz}$		$-\alpha A_{yy}$			A_{yy}
$\lvert T_x;-\frac{1}{2}\rangle$	H			$-D_{xx}-Q$				$1/2iA_{zz}$		αA_{yy}	$-A_{yy}$	
$\lvert T_y;+\frac{3}{2}\rangle$	$3/2iA_{zz}$				$-D_{yy}+Q$			H			$-i\alpha A_{xx}$	
$\lvert T_y;-\frac{3}{2}\rangle$		$-3/2iA_{zz}$				$-D_{yy}+Q$	H					$-i\alpha A_{xx}$
$\lvert T_y;+\frac{1}{2}\rangle$			$1/2iA_{zz}$			H	$-D_{yy}-Q$		$-i\alpha A_{xx}$			$-iA_{xx}$
$\lvert T_y;-\frac{1}{2}\rangle$				$-1/2iA_{zz}$	H			$-D_{yy}-Q$		$-i\alpha A_{xx}$	$-iA_{xx}$	
$\lvert T_z;+\frac{3}{2}\rangle$			$-\alpha A_{yy}$				$i\alpha A_{xx}$		$-D_{zz}+Q$			H
$\lvert T_z;-\frac{3}{2}\rangle$				αA_{yy}				$i\alpha A_{xx}$		$-D_{zz}+Q$	H	
$\lvert T_z;+\frac{1}{2}\rangle$	αA_{yy}			$-A_{yy}$	$i\alpha A_{xx}$			iA_{xx}		H	$-D_{zz}-Q$	
$\lvert T_z;-\frac{1}{2}\rangle$		$-\alpha A_{yy}$	A_{yy}			$i\alpha A_{xx}$	iA_{xx}		H			$-D_{zz}-Q$

positions and relative intensities of the allowed and forbidden transitions. When comparing the observed zero-field spectra at low- [Fig. 1(b)] and high-microwave power [Fig. 1(a)] with this diagram we can understand the disappearance of the structure of the 4.3-GHz transition as well as the broadening of the 6.5-GHz transition with increasing microwave power. This arises from the relative increase of the intensities of the forbidden transitions due to saturation of the allowed transitions. With the scheme in Fig. 4 we can also explain the splitting of the transitions observed in the double-resonance experiments. When using cw microwaves at 4300 MHz the $|T_y;\pm\frac{1}{2}\rangle$ and the $|T_z;\pm\frac{1}{2}\rangle$ levels will be connected so that only a transition between the $|T_x;\pm\frac{1}{2}\rangle$ and the $|T_y;\pm\frac{1}{2}\rangle$ sublevels at 2260 MHz can be induced. The same argument applies for the transitions between the $m_I=\pm\frac{3}{2}$ sublevels, and it will give rise to the observation of the 2200-MHz (T_x-T_y) transition when the 4350-MHz (T_y-T_z) transition is subjected to cw microwaves.

The values of the different parameters $D_{ii}, P_{z'z'}, \eta$, and A, as well as the choice of the direction of the quadrupole principal axes deserve a few comments. First we note that the observed zero-field frequencies are not determined entirely by D_{ii} but partly by the second-order shift of the levels induced by the hyperfine interaction A. Second it appears from the diagonalization procedure that the splitting of the $m_I=\pm\frac{1}{2}$ and $\pm\frac{3}{2}$ substates is different for each triplet sublevel. This difference, which gives rise to the doublet structure, is predominantly determined by the second-order hyperfine interaction. The consequence is that the accuracy in the value of A (175±20 MHz) is considerably higher than that for the quadrupole splitting. So far we can only say that the quadrupole splitting parameter $P_{z'z'}$ is between 10 and 20 MHz. If $P_{z'z'}>20$ MHz the ordering of the nuclear sublevels is incorrect, whereas for $P_{z'z'}<10$ MHz the probability for the forbidden transitions will become too small. Further we find that the fitting procedure neither gives a preference for the direction of the quadrupole principal axes x',y',z' with respect to the axes x,y,z of the zero-field tensor, nor does it give a preference for a value for η. We expect, however, that $\eta\neq 0$ due to the low symmetry of the defect as deduced from the X-band ODMR experiments.[6,7]

The neglect of the difference between the two Cu isotopes can now also be justified. From the difference of 7% in the nuclear g values we conclude that the second-order shift induced by the hyperfine coupling constant would yield a difference of 1–2 MHz for the zero-field transitions of the two isotopes; clearly this value is too small to be observable. The same argument holds for the quadrupole coupling constant. Here the difference of the quadrupole moments would lead to a maximum splitting of only 1–2 MHz.

For the analysis of the line shape of the three zero-field transitions of the S_B triplet a similar procedure was followed. The best-fit parameters and the corresponding eigenenergies and eigenfunctions are found in Tables II and IV respectively. Here the second-order energy shift of the nuclear sublevels is a factor of 1.5–2 larger than for S_A since the zero-field splitting frequencies are smaller by the same factor. (The hyperfine interaction A is estimated to be the same as for S_A from the observation that the ODMR transitions in the presence of a magnetic field exhibit a similar linewidth.)

TABLE II. The set of best parameters resulting from the fitting procedure for S_A and S_B, respectively. For S_A z is 17° off the [111] axis towards the [001] axis in the $(1\bar{1}0)$ plane, y is parallel to $[1\bar{1}0]$, and x is perpendicular to both y and z. For S_B the z axis is parallel to [111] but the directions of x and y are still unknown.

	D_{xx} (MHz)	D_{yy} (MHz)	D_{zz} (MHz)	A (MHz)	$P_{z'z'}$ (MHz)	η
S_A	−2905	−705	3610	175	10–20	0–1
S_B	−1295	−180	1475	175	30–40	1

TABLE III. The eigenfunctions $|T_u;m_I\rangle'$ for the triplet sublevels of S_A as resulting from the fit procedure. The parameters used are found in Table II. Further we have chosen $P_{z'z'}=12$ MHz, $\eta=1$ and z' parallel to x. In the first column only the functions $|T_u;+\frac{3}{2}\rangle'$ and $|T_u;+\frac{1}{2}\rangle'$ are given. The expressions for the functions $|T_u;-\frac{3}{2}\rangle'$ and $|T_u;-\frac{1}{2}\rangle'$ can be found by interchanging the columns headed by $+m_I$ and $-m_I$.

S_A		Basis functions											
		T_x				T_y				T_z			
Eigenfunctions	Eigenenergy (MHz)	$+\frac{3}{2}$	$-\frac{3}{2}$	$+\frac{1}{2}$	$-\frac{1}{2}$	$+\frac{3}{2}$	$-\frac{3}{2}$	$+\frac{1}{2}$	$-\frac{1}{2}$	$+\frac{3}{2}$	$-\frac{3}{2}$	$+\frac{1}{2}$	$-\frac{1}{2}$
$\|T_x;+\frac{3}{2}\rangle'$	2919.4	0.81			−0.59		0.04i	−0.01i			0.01	−0.04	
$\|T_x;+\frac{1}{2}\rangle'$	2935.8		0.59	0.80		−0.05i			−0.10i	0.02			−0.01
$\|T_y;+\frac{3}{2}\rangle'$	720.5		0.02i	−0.04i		0.97			−0.25	−0.06i			
$\|T_y;+\frac{1}{2}\rangle'$	674.2	−0.07i			−0.09i		0.24	0.96			0.02i	−0.02i	
$\|T_z;+\frac{3}{2}\rangle'$	−3629.5	0.02			−0.04		−0.04i	−0.02i			−0.62	0.79	
$\|T_z;+\frac{1}{2}\rangle'$	−3620.4		−0.01			−0.05i			0.01i	0.79			0.62

The remarkable difference from S_A is the absence of a doublet structure. We think that this results from two effects. First the quadrupole splitting parameter $P_{z'z'}$ is larger than for S_A (30 MHz $<P_{z'z'}<$ 40 MHz) and in combination with the hyperfine interaction this leads to a heavy mixing of the $m_I=\pm\frac{1}{2}$ and $\pm\frac{3}{2}$ sublevels. Consequently forbidden and allowed lines acquire about the same transition probability as can be seen in the stick diagram of Fig. 2. Second the inhomogeneous linewidth of each transition is about a factor of 2 larger than for S_A (100 MHz vs 50 MHz). These two effects together wash out the expected structure. Again we find that the fitting is rather insensitive to the direction of the quadrupole principal axis.

The estimate of the inhomogeneous linewidths is based on the following arguments. From the fitting procedure it can be seen that the T_x-T_z transitions are always composed of two strong allowed lines almost at the same frequency and two forbidden lines at higher and lower frequencies, respectively (see the stick diagrams of Figs. 2(c) and 1, 6.55 GHz). The observed linewidths for these transitions therefore should be very close to the inhomogeneous linewidth of each transition between nuclear substates. This conclusion agrees very well with the observed linewidths for S_A as well as with the inhomogeneous linewidth that had to be used for a proper fit of the S_B spectra.

The finding that the quadrupole splitting parameter $P_{z'z'}$ for S_B is about two times larger than for S_A is an indication that the surroundings of the Cu atom changes when going from S_A to S_B and vice versa. Here we have to realize that the electric-field gradient, which determines the size of the quadrupole splitting parameter, reflects the influence of the direct surrounding of the Cu atom. Since we believe that the sulfur atoms remain on the same substitutional lattice positions, we conclude that the Cu atom changes its position in the defect during the conversion. The observation that the inhomogeneous linewidth differs by a factor of 2 between S_A and S_B seems to support this model. Apparently in the case of S_B the Cu atom occupies a position that leads to a larger variation in local strain. At present it does not seem possible to give any specific indication about the locations of the Cu atom. An answer to this question should come from ENDOR measurements.

V. CONCLUSIONS

From an analysis of the line shapes of the zero-field ODMR spectra of the excited triplet states of the two

TABLE IV. The eigenfunctions $|T_u;m_I\rangle'$ for the triplet sublevels of S_B as resulting from the fit procedure. The parameters are found in Table II. Further we have chosen $P_{z'z'}=40$ MHz, $\eta=1$, and z' parallel to x. In the first column only the functions $|T_u;+\frac{3}{2}\rangle'$ and $|T_u;+\frac{1}{2}\rangle'$ are given. The expressions for the functions $|T_u;-\frac{3}{2}\rangle'$ and $|T_u;-\frac{1}{2}\rangle'$ can be found by interchanging the columns headed by $+m_I$ and $-m_I$.

S_B		Basis functions											
		T_x				T_y				T_z			
Eigenfunctions	Eigenenergy (MHz)	$+\frac{3}{2}$	$-\frac{3}{2}$	$+\frac{1}{2}$	$-\frac{1}{2}$	$+\frac{3}{2}$	$-\frac{3}{2}$	$+\frac{1}{2}$	$-\frac{1}{2}$	$+\frac{3}{2}$	$-\frac{3}{2}$	$+\frac{1}{2}$	$-\frac{1}{2}$
$\|T_x;+\frac{3}{2}\rangle'$	1364.0	0.75			−0.63		0.08	−0.19			0.03i	−0.01i	
$\|T_x;+\frac{1}{2}\rangle'$	1315.0		0.65	0.75		0.10			−0.02	−0.03i			−0.08i
$\|T_y;+\frac{3}{2}\rangle'$	226.4		−0.01	−0.11		0.98			0.07	0.16i			0.01i
$\|T_y;+\frac{1}{2}\rangle'$	120.0	0.13			−0.14		−0.06	0.98			0.02i	0.06i	
$\|T_z;+\frac{3}{2}\rangle'$	−1489.1		0.03i	−0.01i		0.12i			0.03i	0.79			−0.60
$\|T_z;+\frac{1}{2}\rangle'$	−1536.2	−0.04i			−0.09i		−0.10i	−0.05i			0.59	0.79	

configurations 1 and 2 of the sulfur-pair-related defect in silicon it appears that a Cu atom is involved in the complex. This conclusion is based on a model in which the hyperfine interaction between the $S=1$ triplet spin and the $I=\frac{3}{2}$ nuclear spin of Cu, together with the nuclear quadrupole interaction is considered. Further we infer that the quadrupole splitting parameters as well as the inhomogeneous linewidths differ between S_A and S_B, suggesting that the Cu atom occupies different lattice positions in the two configurations of this complex defect. This conclusion agrees with the X-band ODMR data where it is found that the configurations 1 and 2 (corresponding to the two emissions S_A and S_B) have different low symmetry in the neutral charge state. The results of this work demonstrate the power of zero-field ODMR techniques (including double-resonance experiments) to identify the atoms forming part of complex defects in a semiconductorlike silicon, when magnetic resonance in an external magnetic field gives insufficient information about the atomic species in the defect due to unresolved hyperfine interaction.

ACKNOWLEDGMENT

This research was partly supported by the Commission of the European Communities Science Plan via Grant No. SCI-0363-M.

[1]T. G. Brown and D. G. Hall, Appl. Phys. Lett. **49**, 245 (1986).

[2]D. J. S. Beckett, M. K. Nissen, and M. L. W. Thewalt, Phys. Rev. B **40**, 9618 (1989).

[3]M. Singh, E. C. Lightowlers, G. Davies, C. Jeynes, and K. J. Reeson, Mater. Sci. Eng. B **4**, 303 (1989).

[4]A. Henry, W. M. Chen, E. Janzén, and B. Monemar, in *Proceedings of the 20th International Conference on the Physics of Semiconductors, Greece,* edited by E. M. Anastassakis and J. D. Joannopoulos (World Scientific, Singapore, 1990), p. 545.

[5]E. Janzén, R. Stedman, G. Grossmann, and H. G. Grimmeiss, Phys. Rev. B **29**, 1907 (1984).

[6]W. M. Chen, A. Henry, E. Janzén, B. Monemar, and M. L. W. Thewalt, MRS Symposia Proceedings No. 163 (Material Research Society, Pittsburgh, 1990), p. 303.

[7]W. M. Chen, M. Singh, A. Henry, E. Janzén, B. Monemar, A. M. Frens, M. T. Bennebroek, J. Schmidt, K. J. Reeson, and R. M. Gwillian, Mater. Sci. Forum **83-87**, 251 (1992).

[8]L. E. Erickson, Phys. Rev. **143**, 295 (1966).

[9]T. Moreno, *Microwave Transmission Design Data* (McGraw-Hill, New York, 1948).

[10]W. M. Chen and B. Monemar, J. Appl. Phys. **68**, 2506 (1990).

[11]A. M. Frens, M. T. Bennebroek, and J. Schmidt (unpublished).

[12]J. Schmidt and J. H. van der Waals, Chem. Phys. Lett. **3**, 546 (1969).

[13]E. R. Weber, Appl. Phys. **A30**, 1 (1983).

[14]H. W. de Wijn and J. L. de Wildt, Phys. Rev. **150**, 200 (1966).